Measurement of the SM Higgs boson mass in the diphoton and four-lepton decay channels using the ATLAS detector

Marcello Fanti (University of Milano and INFN)

(on behalf of the ATLAS collaboration)

Bibliography

ATLAS-CONF-2017-046
"Measurement of the Higgs boson mass in the $H \to ZZ^* \to 4\ell$ and $H \to \gamma\gamma$ channels with $\sqrt{s} = 13\ \mathrm{TeV}$ pp collisions using the ATLAS detector"

Importance of mass measurement

In the Standard Model, m_H is the only free parameter of the Higgs sector

The Higgs sector has two parameters: μ and λ related to the VEV v and the Higgs mass m_H by: $\mu = \frac{m_H}{\sqrt{2}}$ and $\lambda = \frac{1}{2}\left(\frac{m_H}{v}\right)^2$. Since $v = \sqrt{\frac{1}{\sqrt{2}\,G_F}}$ is known, m_H is the only free parameter.

cross-section

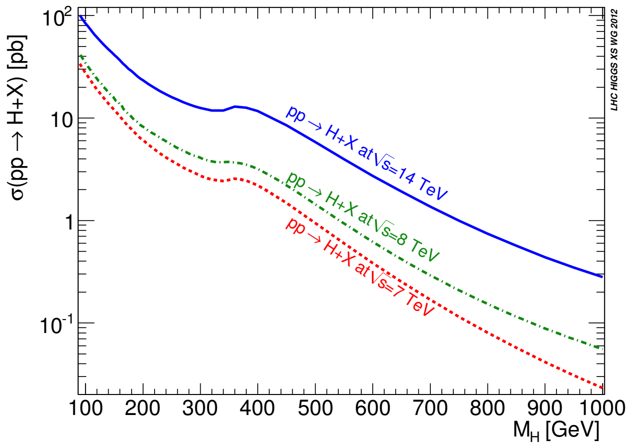

decay width

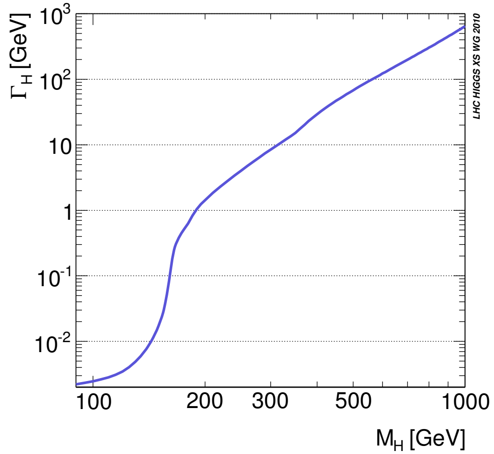

branching ratios

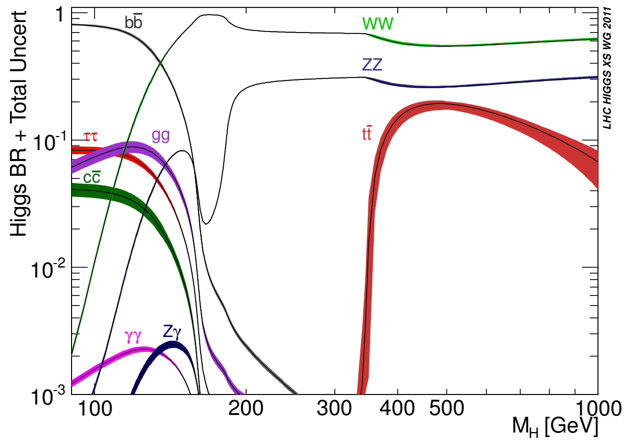

⇒ everything else is calculable, once m_H is given.

[https://twiki.cern.ch/twiki/bin/view/LHCPhysics/CERNYellowReportPageBR]

Decay channels for mass measurement

$H \to 4\ell$

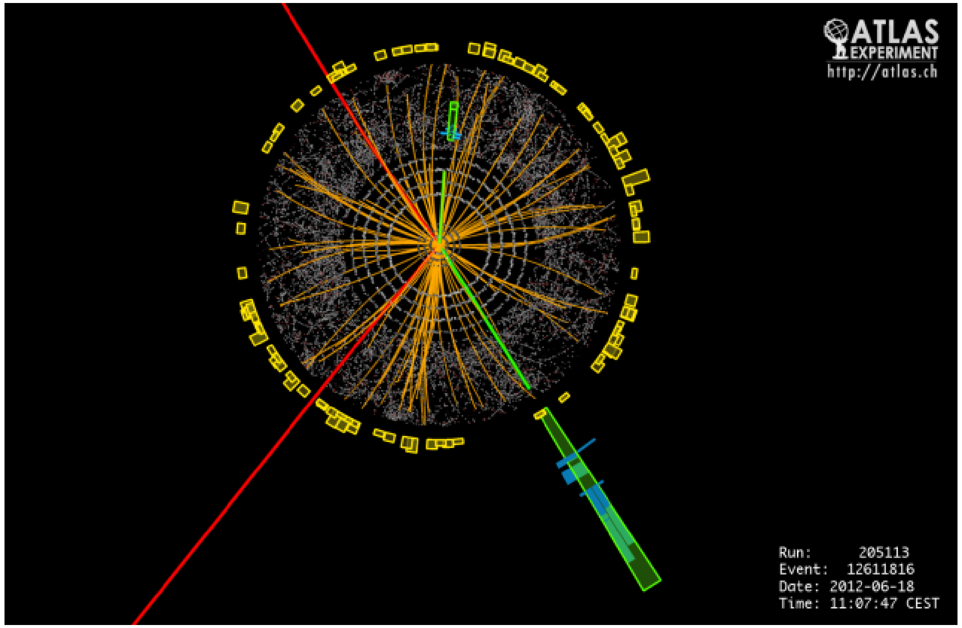

PRO : good signal/background ratio $\sim 1/1$
CON : only ~ 100 events

$H \to \gamma\gamma$

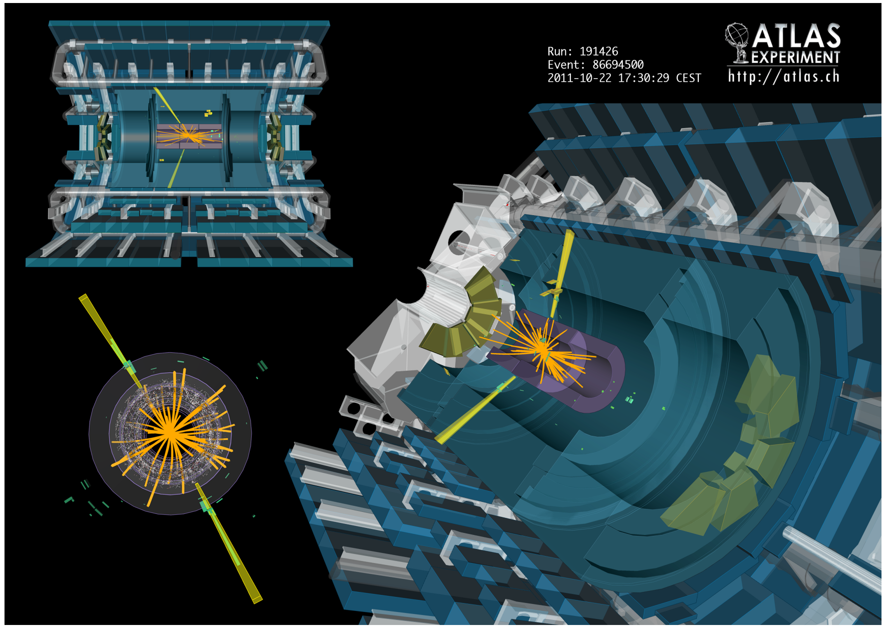

PRO : higher statistics
CON : signal/background $\sim 2\%$

The full final state is reconstructed, and measured with high energy precision.

$\Rightarrow$ invariant mass can be measured with $\mathcal{O}\left(1 \text{ GeV}\right)$ resolution

Energy calibration

Calibration

Simulation is accurate, but residual details impact the energy scale and resolution:

- for muons: energy loss in material, B-field description, detector geometry, misalignments
- for electrons/photons: energy loss before the EM calorimeter (ECAL), shower modelling, layers intercalibration

Calibration

Simulation is accurate, but residual details impact the energy scale and resolution:

- for muons: energy loss in material, B-field description, detector geometry, misalignments
- for electrons/photons: energy loss before the EM calorimeter (ECAL), shower modelling, layers intercalibration

Muon calibration

Data-driven p_{T} corrections derived from $J/\psi \to \mu^+\mu^-$ and $Z \to \mu^+\mu^-$

$$\delta p_{\mathrm{T}} = \sum_k c_k(\eta, \phi)(p_{\mathrm{T}})^k$$

Corrected MC is checked against data in $Z \to \mu^+\mu^-$ decays

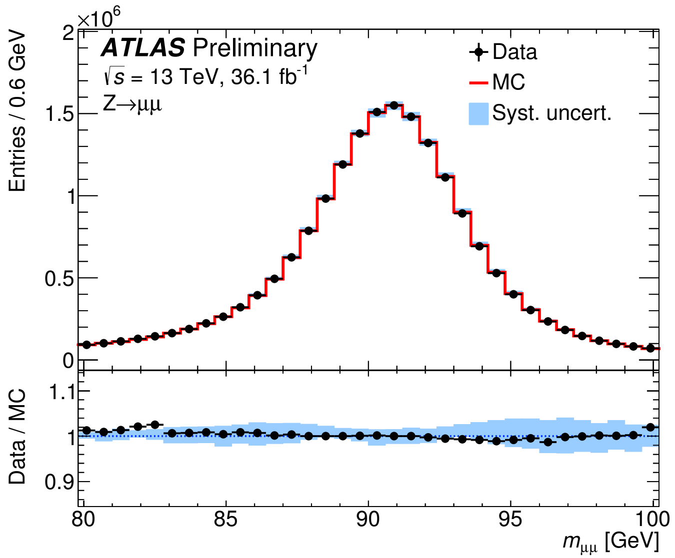

Calibration

Simulation is accurate, but residual details impact the energy scale and resolution:

- for muons: energy loss in material, B-field description, detector geometry, misalignments
- for electrons/photons: energy loss before the EM calorimeter (ECAL), shower modelling, layers intercalibration

Electron/photon calibration

Energy deposited in EM cluster is corrected for:

- energy loss upstream the ECAL
- lateral leakage out of cluster
- leakage beyond the ECAL
- impact point in the ECAL

All correction are optimized on simulation, separately for electrons, unconverted photons, converted photons, with a BDT technique.
Intercalibration of ECAL layers checked with muons.
Material in front of ECAL checked with electron longitudinal shower shape
Energy scale adjustments (as functions of η) are derived from $Z \to e^+e^-$

Calibration

Simulation is accurate, but residual details impact the energy scale and resolution:

- for muons: energy loss in material, B-field description, detector geometry, misalignments
- for electrons/photons: energy loss before the EM calorimeter (ECAL), shower modelling, layers intercalibration

Electron/photon calibration

Energy deposited in EM cluster is corrected for:

- energy loss upstream the ECAL
- lateral leakage out of cluster
- leakage beyond the ECAL
- impact point in the ECAL

All correction are optimized on simulation, separately for electrons, unconverted photons, converted photons, with a BDT technique.

Intercalibration of ECAL layers checked with muons.

Material in front of ECAL checked with electron longitudinal shower shape

Energy scale adjustments (as functions of η) are derived from $Z \to e^+e^-$

for electrons:

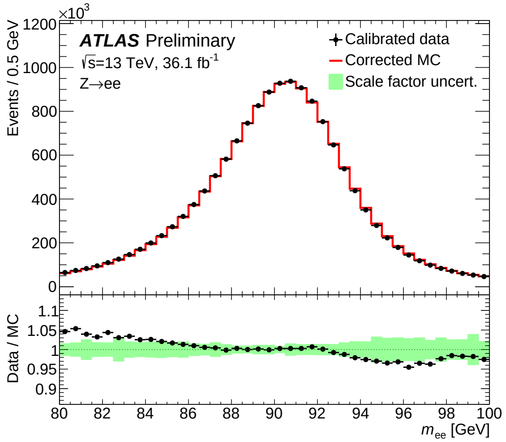

checked on $Z \to e^+e^-$

Calibration

Simulation is accurate, but residual details impact the energy scale and resolution:

- for muons: energy loss in material, B-field description, detector geometry, misalignments
- for electrons/photons: energy loss before the EM calorimeter (ECAL), shower modelling, layers intercalibration

Electron/photon calibration

Energy deposited in EM cluster is corrected for:

- energy loss upstream the ECAL
- lateral leakage out of cluster
- leakage beyond the ECAL
- impact point in the ECAL

All correction are optimized on simulation, separately for electrons, unconverted photons, converted photons, with a BDT technique.

Intercalibration of ECAL layers checked with muons.

Material in front of ECAL checked with electron longitudinal shower shape

Energy scale adjustments (as functions of η) are derived from $Z \to e^+e^-$

for electrons:

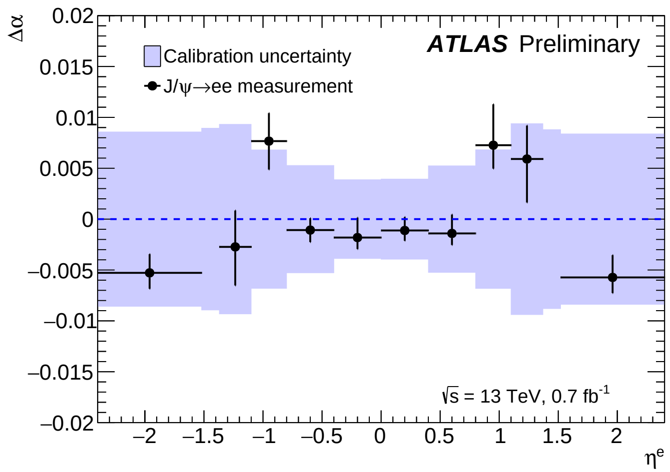

... and on $J/\psi \to e^+e^-$

Calibration

Simulation is accurate, but residual details impact the energy scale and resolution:

- for muons: energy loss in material, B-field description, detector geometry, misalignments
- for electrons/photons: energy loss before the EM calorimeter (ECAL), shower modelling, layers intercalibration

Electron/photon calibration

Energy deposited in EM cluster is corrected for:

- energy loss upstream the ECAL
- lateral leakage out of cluster
- leakage beyond the ECAL
- impact point in the ECAL

All correction are optimized on simulation, separately for electrons, unconverted photons, converted photons, with a BDT technique.

Intercalibration of ECAL layers checked with muons.

Material in front of ECAL checked with electron longitudinal shower shape

Energy scale adjustments (as functions of η) are derived from $Z \to e^+e^-$

for photons:

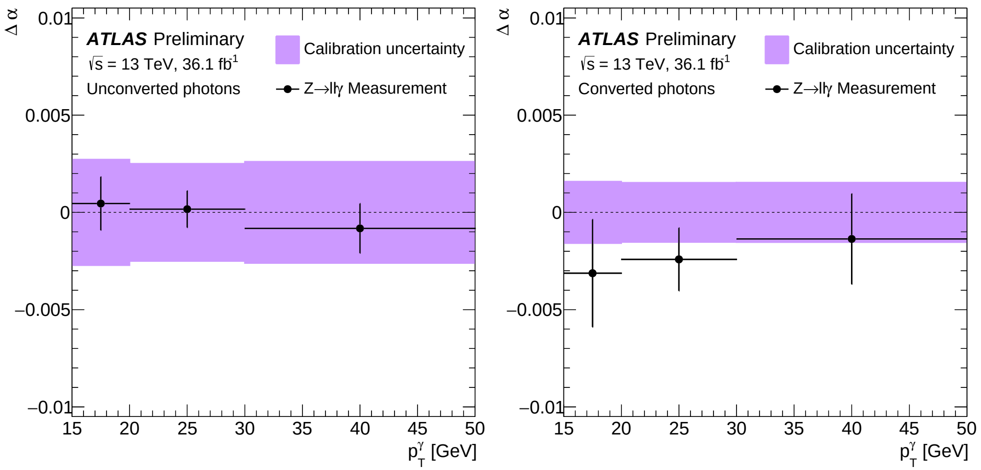

checked on $Z \to \ell\ell\gamma$

Measurement in $H \to 4\ell$ channel

Event selection

Select 4-lepton events of the type $\ell_1^+\ell_1^-\ell_2^+\ell_2^-$ — "leading" $\ell\ell$-pair is that with $m_{\ell\ell}$ closest to m_Z.

$m_{\ell\ell}^{(lead)} \in [50; 106]\ \mathrm{GeV}$ — constrained to m_Z in final fit
$m_{\ell\ell}^{(sublead)} > 12\ \mathrm{GeV}$

$m_{4\ell} \in [110; 135]\ \mathrm{GeV}$

Leptons must pass identification and isolation criteria.

Event selection

Select 4-lepton events of the type $\ell_1^+\ell_1^-\ell_2^+\ell_2^-$ — "leading" $\ell\ell$-pair is that with $m_{\ell\ell}$ closest to m_Z.

$m_{\ell\ell}^{(lead)} \in [50; 106]$ GeV — constrained to m_Z in final fit
$m_{\ell\ell}^{(sublead)} > 12$ GeV

$m_{4\ell} \in [110; 135]$ GeV

Leptons must pass identification and isolation criteria.

Events are classified by flavour of $(\ell\ell)^{(lead)}$ and $(\ell\ell)^{(sublead)}$

Final state	Signal (125 GeV)	ZZ^*	Z + jets, $t\bar{t}$, WZ, ttV,VVV	Expected	Observed
4μ	20.6 ± 1.7	15.9 ± 1.2	2.0 ± 0.4	38.5 ± 2.1	38
$2e2\mu$	14.6 ± 1.1	11.2 ± 0.8	1.6 ± 0.4	27.5 ± 1.4	34
$2\mu 2e$	11.2 ± 1.0	7.4 ± 0.7	2.2 ± 0.4	20.8 ± 1.3	26
$4e$	11.1 ± 1.1	7.1 ± 0.7	2.1 ± 0.4	20.3 ± 1.3	24
Total	57 ± 5	41.6 ± 3.2	8.0 ± 1.0	107 ± 6	122

Event selection

Select 4-lepton events of the type $\ell_1^+\ell_1^-\ell_2^+\ell_2^-$ — “leading” $\ell\ell$-pair is that with $m_{\ell\ell}$ closest to m_Z.

$m_{\ell\ell}^{(lead)} \in [50;106]\ \mathrm{GeV}$ — constrained to m_Z in final fit
$m_{\ell\ell}^{(sublead)} > 12\ \mathrm{GeV}$

$m_{4\ell} \in [110;135]\ \mathrm{GeV}$

Leptons must pass identification and isolation criteria.

Events are classified by flavour of $(\ell\ell)^{(lead)}$ and $(\ell\ell)^{(sublead)}$

Final state	Signal (125 GeV)	ZZ^*	$Z+\mathrm{jets}, t\bar{t}, WZ, ttV, VVV$	Expected	Observed
4μ	20.6 ± 1.7	15.9 ± 1.2	2.0 ± 0.4	38.5 ± 2.1	38
$2e2\mu$	14.6 ± 1.1	11.2 ± 0.8	1.6 ± 0.4	27.5 ± 1.4	34
$2\mu 2e$	11.2 ± 1.0	7.4 ± 0.7	2.2 ± 0.4	20.8 ± 1.3	26
$4e$	11.1 ± 1.1	7.1 ± 0.7	2.1 ± 0.4	20.3 ± 1.3	24
Total	57 ± 5	41.6 ± 3.2	8.0 ± 1.0	107 ± 6	122

Discrimination between $H \to ZZ^* \to 4\ell$ and irreducible background $ZZ \to 4\ell$ is achieved through a BDT score with inputs:

$$p_{\mathrm{T}}^{4\ell} \quad , \quad \eta^{4\ell} \quad , \quad \mathcal{D}_{ZZ^*} \equiv \ln\left(\frac{|\mathcal{M}_{H\to ZZ^*}|^2}{|\mathcal{M}_{ZZ}|^2}\right)$$

$\Rightarrow$ 16 event categories : (4 lepton-flavour categories) $\otimes$ (4 BDT score bins)

Signal & background models

Signal

Invariant mass pdf $S(m_{4\ell})$ obtained per-event as $S(m_{4\ell}) = \int dm_{4\ell}^{(true)} \cdot F(m_{4\ell} - m_{4\ell}^{(true)}) \cdot BW(m_{4\ell}^{(true)} | m_H)$

Experimental response function $F(m_{4\ell} - m_{4\ell}^{(true)})$ depends on energy response functions of the 4 leptons (depending on lepton flavour, η, p_{T}).

Each energy response is modeled by 3 Gaussians $\Rightarrow$ convolution of $3^4 = 81$ Gaussians

$\Rightarrow$ further reduced to 4 Gaussians that mimic at best the complete parametrization

Signal & background models

Signal

Invariant mass pdf $S(m_{4\ell})$ obtained per-event as $S(m_{4\ell}) = \int dm_{4\ell}^{(true)} \cdot F(m_{4\ell} - m_{4\ell}^{(true)}) \cdot BW(m_{4\ell}^{(true)} | m_H)$

Experimental response function $F(m_{4\ell} - m_{4\ell}^{(true)})$ depends on energy response functions of the 4 leptons (depending on lepton flavour, η, p_{T}).
Each energy response is modeled by 3 Gaussians $\Rightarrow$ convolution of $3^4 = 81$ Gaussians
$\Rightarrow$ further reduced to 4 Gaussians that mimic at best the complete parametrization

Background

- **irreducible** $ZZ \to 4\ell$:
  NLO simulation, scaled to NNLO calculation
- **reducible** (Z+jets, $t\bar{t}$, WZ processes):
  LO or NLO simulation, scaled to data control regions, obtained by relaxing the isolation and inverting the impact parameter requirement, on the subleading $\ell\ell$ pair.

$H \to 4\ell$: invariant mass spectra

inclusive

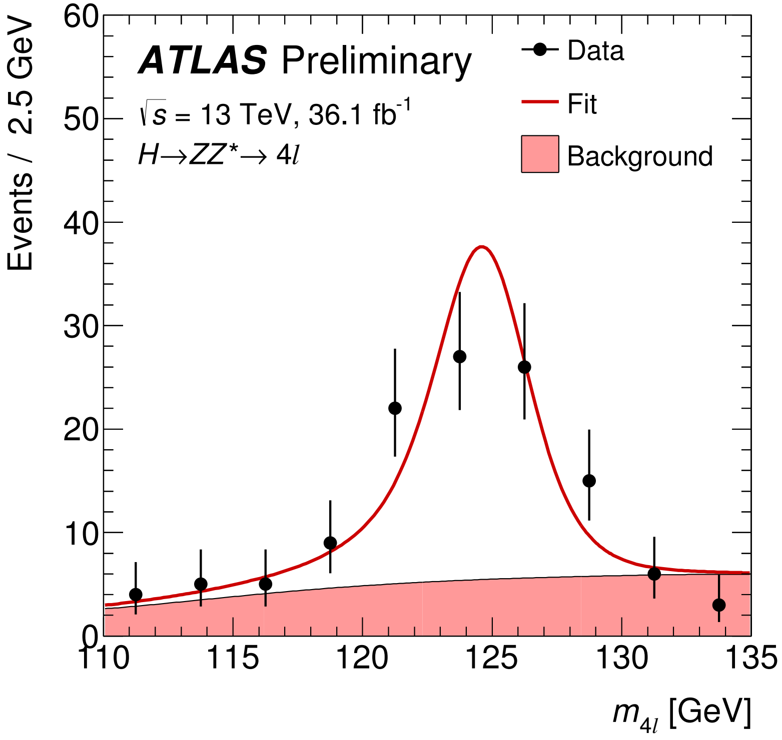

(combined fit over 16 categories)

$H \to 4\mu$

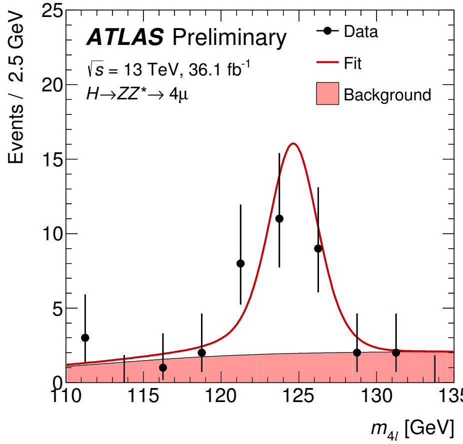

$H \to 2e2\mu$

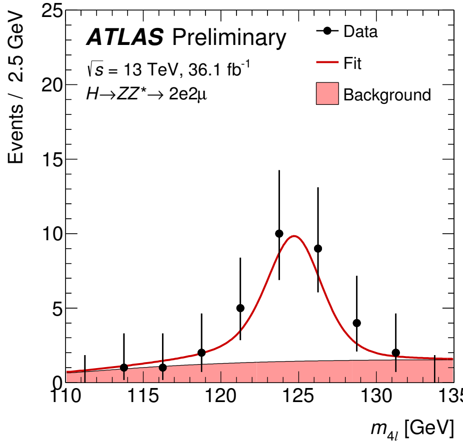

$H \to 2\mu 2e$

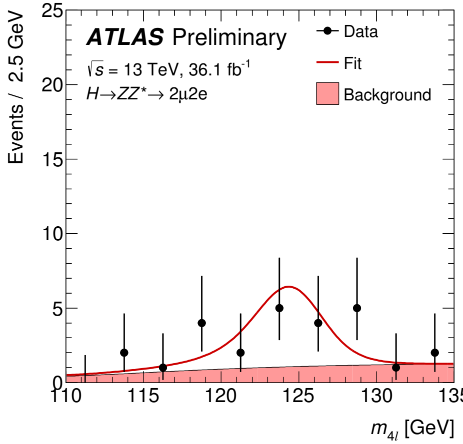

$H \to 4e$

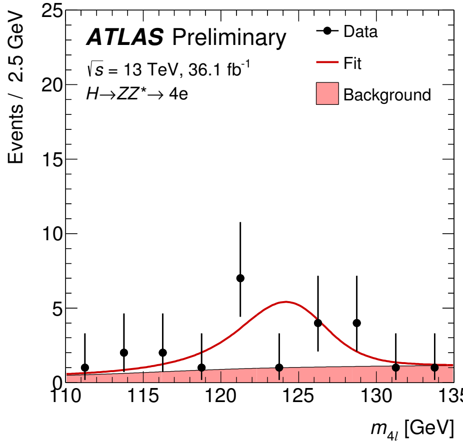

Fit of m_H in the $H \to 4\ell$ channels

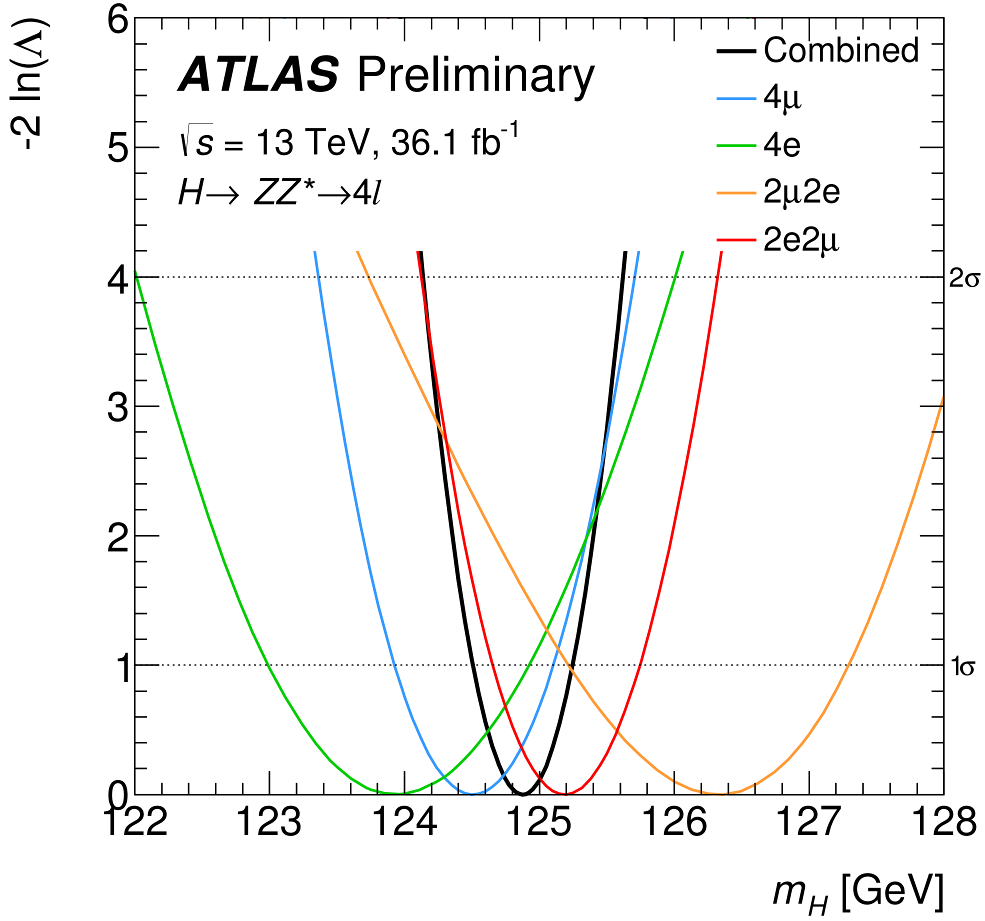

Fit of m_H in the $H \to 4\ell$ channels

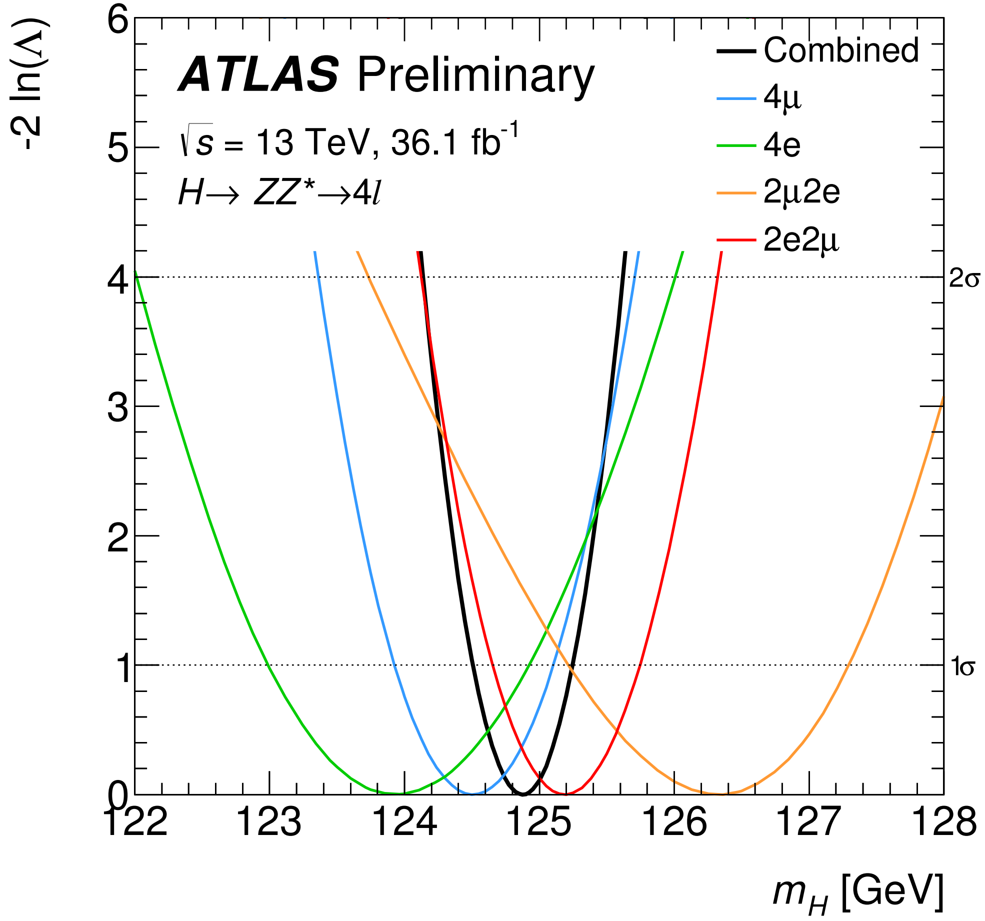

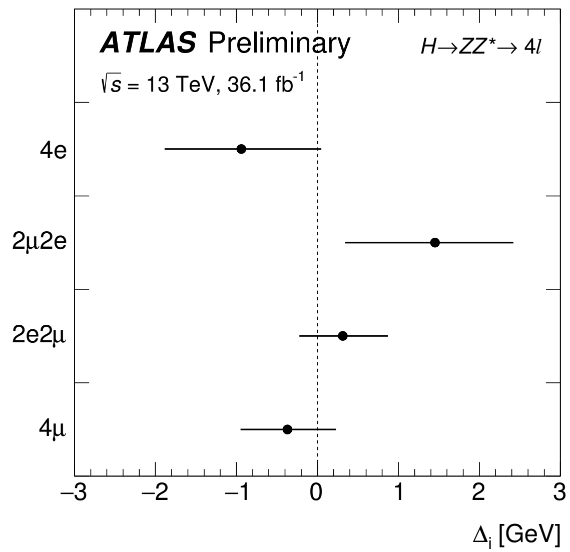

Systematic effect	Uncertainty on $m_H^{ZZ^*}$ [MeV]
Muon momentum scale	40
Electron energy scale	20
Background modelling	10
Simulation statistics	8

$\Rightarrow$ best channels are 4μ and $2e2\mu$ — where subleading $\ell\ell$ pair is $\mu\mu$ (leading $\ell\ell$ pair is always constrained to m_Z)

Fit of m_H in the $H \to 4\ell$ channels

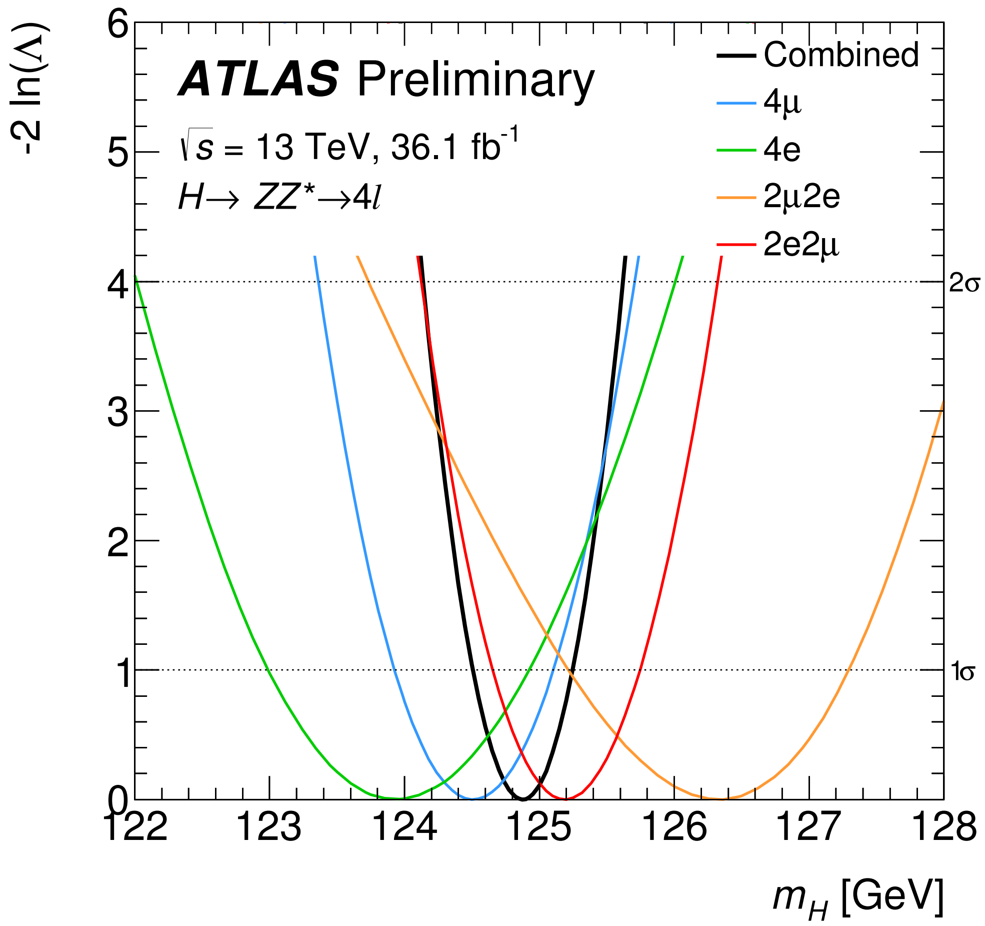

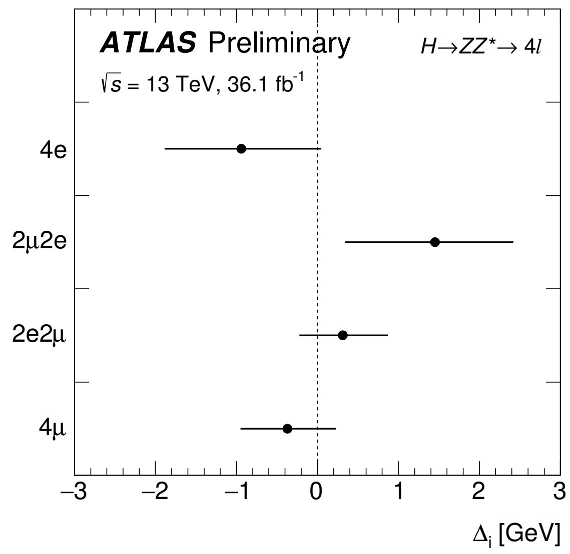

Systematic effect	Uncertainty on $m_H^{ZZ^*}$ [MeV]
Muon momentum scale	40
Electron energy scale	20
Background modelling	10
Simulation statistics	8

⇒ best channels are 4μ and $2e2\mu$ — where subleading $\ell\ell$ pair is $\mu\mu$ (leading $\ell\ell$ pair is always constrained to m_Z)

$$m_H^{(4\ell)} = 124.88 \pm 0.37_{(stat)} \pm 0.05_{(syst)}\ \mathrm{GeV}$$

Measurement in $H \to \gamma\gamma$ channel

Event selection

2 photons passing identification and isolation criteria

$E_{\mathrm{T}}^{(lead)} > 0.35 \cdot m_{\gamma\gamma}$ && $E_{\mathrm{T}}^{(sublead)} > 0.25 \cdot m_{\gamma\gamma}$

Event selection

2 photons passing identification and isolation criteria
$E_{\mathrm{T}}^{(lead)} > 0.35 \cdot m_{\gamma\gamma}$ && $E_{\mathrm{T}}^{(sublead)} > 0.25 \cdot m_{\gamma\gamma}$

Diphoton vertex determined by a NN with inputs:

- photon pointing in ECAL (and possibly in tracker if converted)
- info on primary vertices

(recall: $m_{\gamma\gamma} = \sqrt{E_{\mathrm{T}}^{(lead)} E_{\mathrm{T}}^{(sublead)} (1 - \cos\alpha)}$)
$\Rightarrow$ vertex identification/resolution has negligible impact on $m_{\gamma\gamma}$.

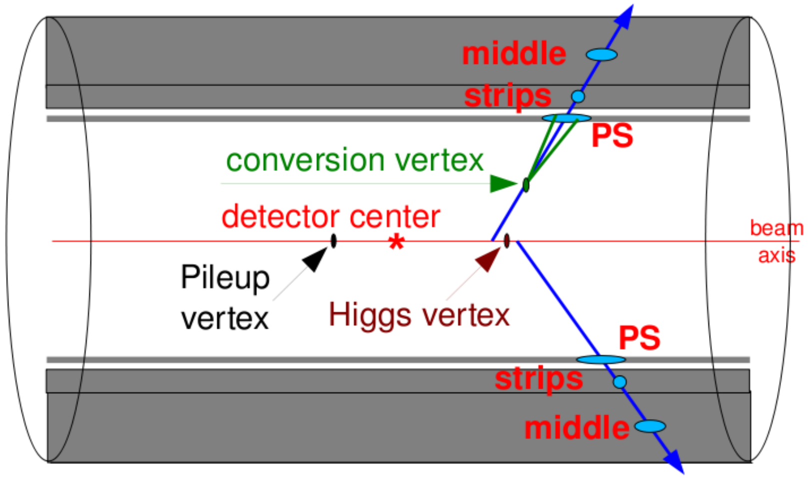

Event selection

2 photons passing identification and isolation criteria
$E_{\rm T}^{(lead)} > 0.35 \cdot m_{\gamma\gamma}$ && $E_{\rm T}^{(sublead)} > 0.25 \cdot m_{\gamma\gamma}$

Diphoton vertex determined by a NN with inputs:

- photon pointing in ECAL (and possibly in tracker if converted)
- info on primary vertices

(recall: $m_{\gamma\gamma} = \sqrt{E_{\rm T}^{(lead)} E_{\rm T}^{(sublead)} (1 - \cos\alpha)}$)
$\Rightarrow$ vertex identification/resolution has negligible impact on $m_{\gamma\gamma}$.

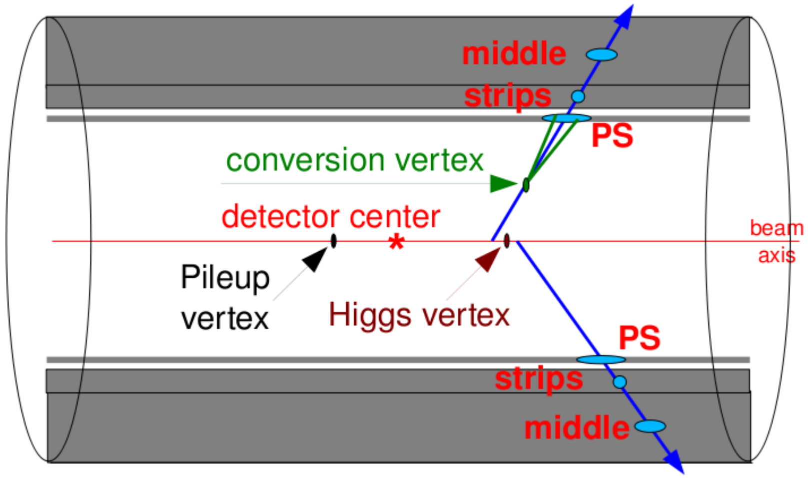

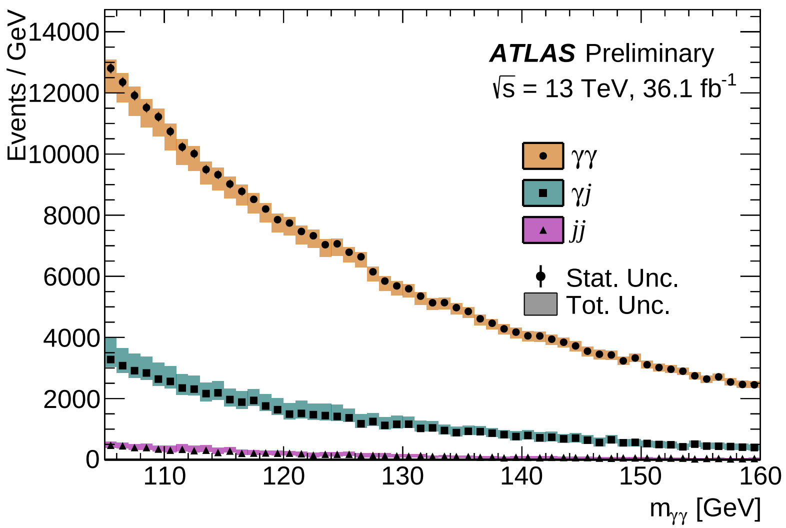

Background: mostly irreducible non-resonant $\gamma\gamma$ (70%–80%)

Background composition ($\gamma\gamma$, γj, jj) estimated by inverting identification and/or isolation

In the following $m_{\gamma\gamma}$ fits, background pdf($m_{\gamma\gamma}$) are modelled by empirical analytical functions, constrained by extending the fit to the sidebands

Event categorization

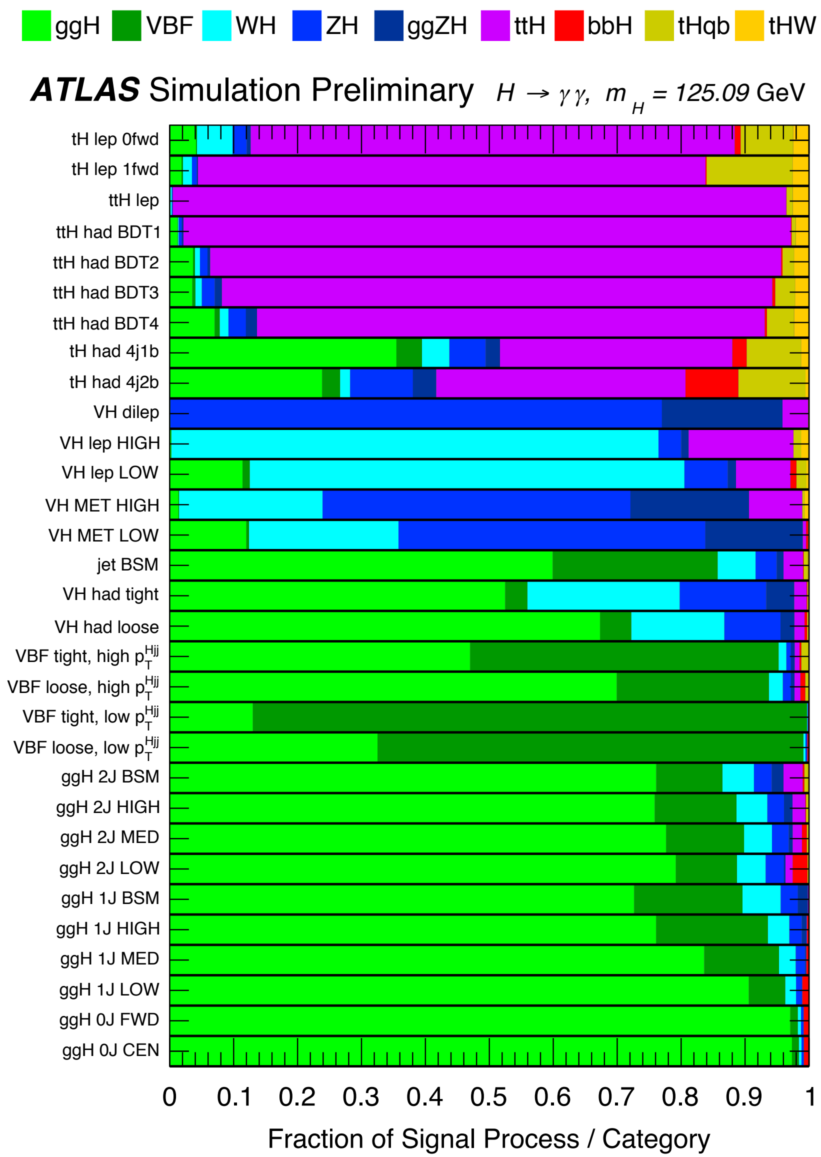

31 categories, chosen to optimize different production modes and improve sensitivity to signal

Event categorization

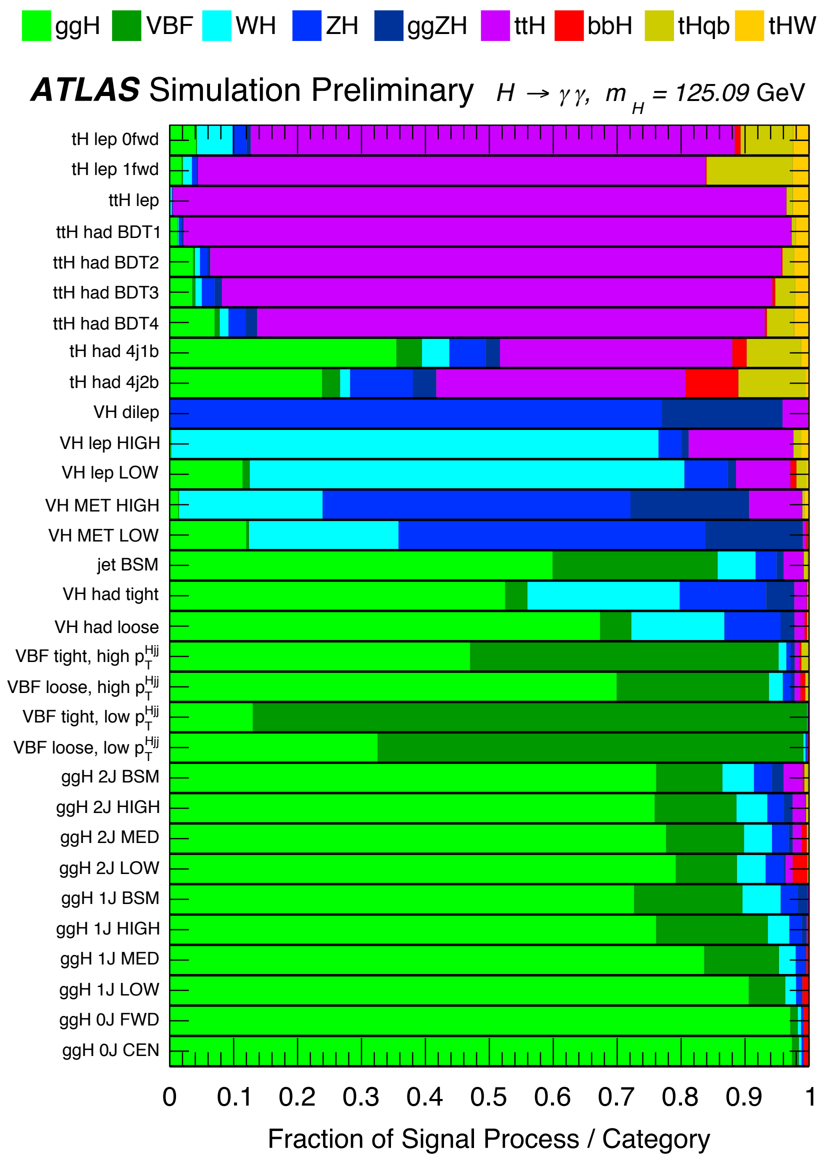

31 categories, chosen to optimize different production modes and improve sensitivity to signal

pdf($m_{\gamma\gamma}$) modelled as 2-sided crystal ball

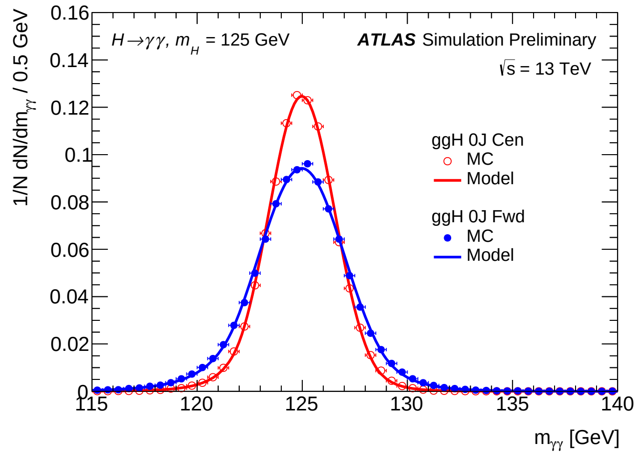

— $\sigma = 1.61$ GeV

— $\sigma = 2.14$ GeV

$\Rightarrow$ 31 different signal models

- same value of m_H
- different Gaussian resolution
- different non-Gaussian tails

$H \rightarrow \gamma\gamma$: invariant mass spectra

ggH categories

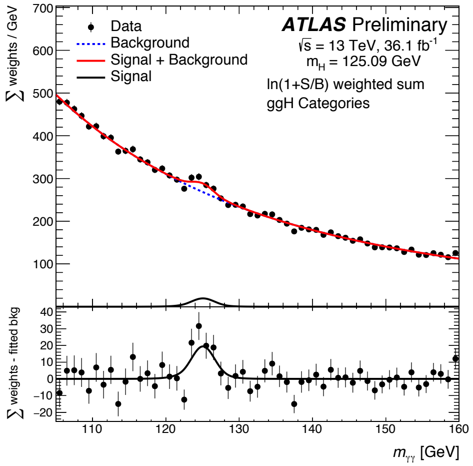

VBF categories

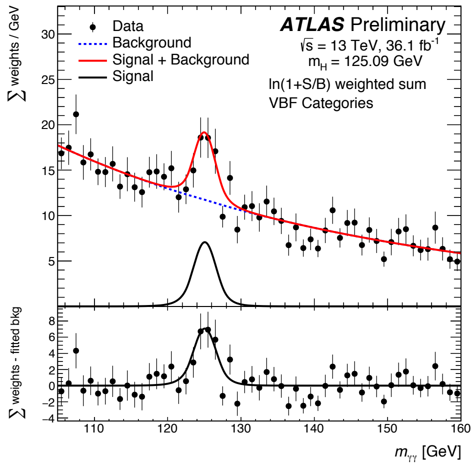

inclusive

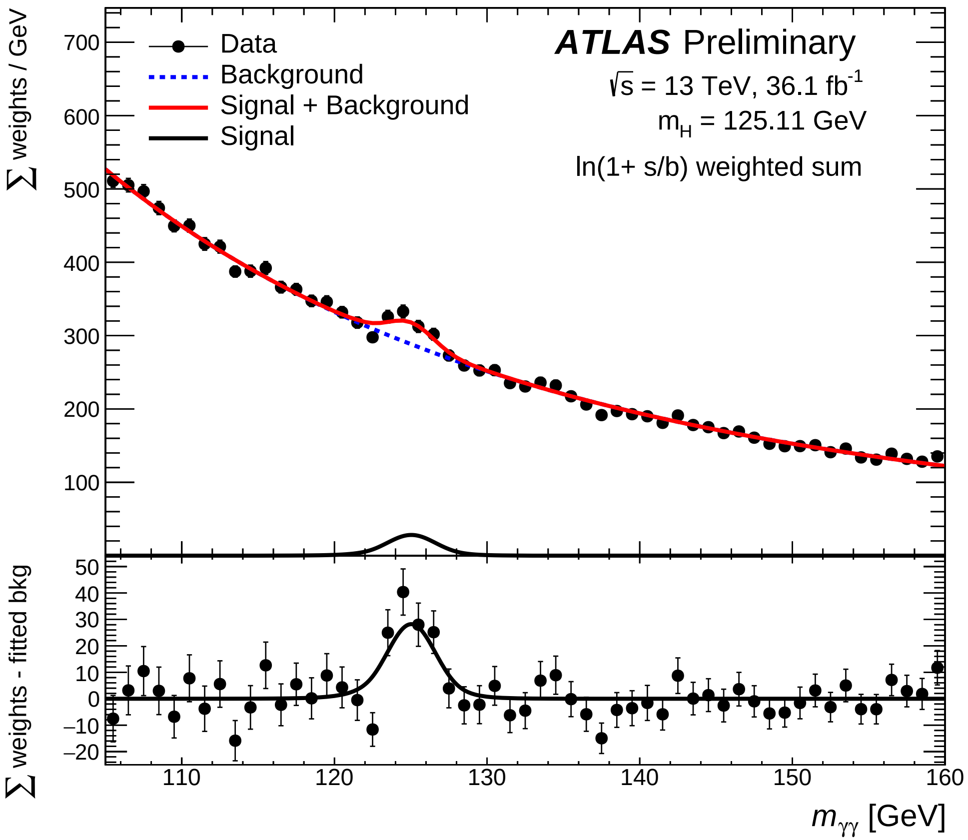

(combined fit over 31 categories)

VH categories

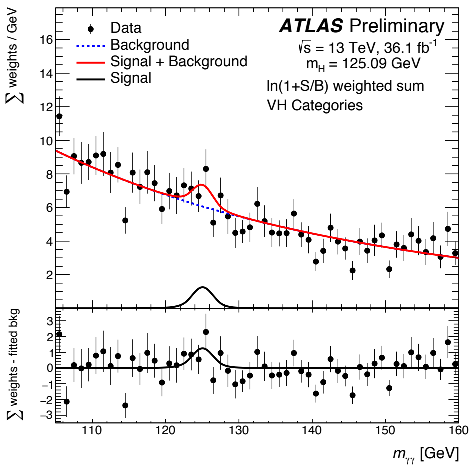

t(t)H categories

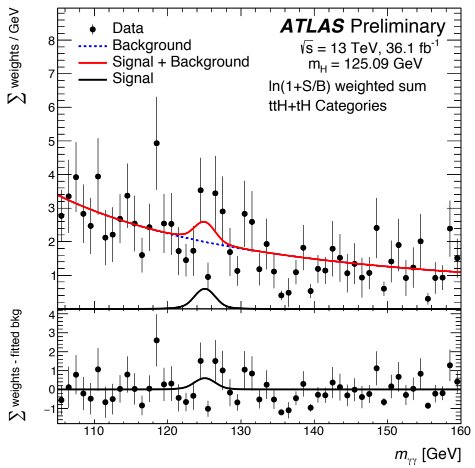

Result for m_H in the $H \to \gamma\gamma$ channels

Source	Systematic uncertainty on $m_H^{\gamma\gamma}$ [MeV]
LAr cell non-linearity	± 200
LAr layer calibration	± 190
Non-ID material	± 120
Lateral shower shape	± 110
ID material	± 110
Conversion reconstruction	± 50
$Z \to ee$ calibration	± 50
Background model	± 50
Primary vertex effect on mass scale	± 40
Resolution	$^{+20}_{-30}$
Signal model	± 20

Result for m_H in the $H \to \gamma\gamma$ channels

Source	Systematic uncertainty on $m_H^{\gamma\gamma}$ [MeV]
LAr cell non-linearity	±200
LAr layer calibration	±190
Non-ID material	±120
Lateral shower shape	±110
ID material	±110
Conversion reconstruction	±50
$Z \to ee$ calibration	±50
Background model	±50
Primary vertex effect on mass scale	±40
Resolution	$^{+20}_{-30}$
Signal model	±20

$$m_H^{(\gamma\gamma)} = 125.11 \pm 0.21_{(stat)} \pm 0.36_{(syst)} \text{ GeV}$$

(expected: $\pm\ 0.25_{(stat)} \pm 0.33_{(syst)}$ GeV)

Result for m_H in the $H \to \gamma\gamma$ channels

Source	Systematic uncertainty on $m_H^{\gamma\gamma}$ [MeV]
LAr cell non-linearity	±200
LAr layer calibration	±190
Non-ID material	±120
Lateral shower shape	±110
ID material	±110
Conversion reconstruction	±50
$Z \to ee$ calibration	±50
Background model	±50
Primary vertex effect on mass scale	±40
Resolution	$^{+20}_{-30}$
Signal model	±20

Cross-checks:

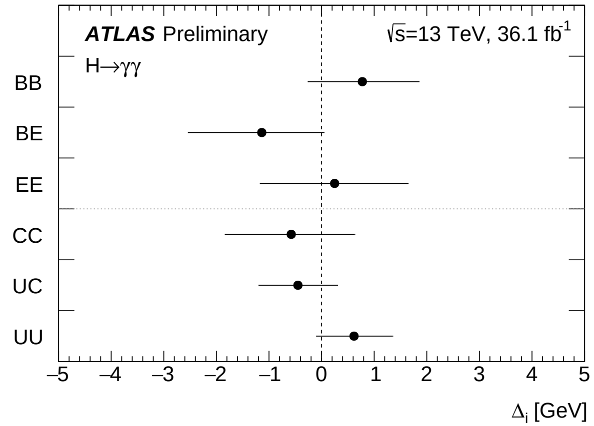

split by barrel/endcap

split by conversion status

$$m_H^{(\gamma\gamma)} = 125.11 \pm 0.21_{(stat)} \pm 0.36_{(syst)} \text{ GeV}$$

(expected: $\pm\ 0.25_{(stat)} \pm 0.33_{(syst)}$ GeV)

Combination

Combination of $H \to 4\ell \oplus H \to \gamma\gamma$

$$m_H^{(4\ell)} = 124.88 \pm 0.37_{(stat)} \pm 0.05_{(syst)} \text{ GeV}$$
$$m_H^{(\gamma\gamma)} = 125.11 \pm 0.21_{(stat)} \pm 0.36_{(syst)} \text{ GeV}$$

$$\Delta m_H = 0.23 \pm 0.42_{(stat)} \pm 0.36_{(syst)} \text{ GeV}$$

Combination of $H \to 4\ell \oplus H \to \gamma\gamma$

$$m_H^{(4\ell)} = 124.88 \pm 0.37_{(stat)} \pm 0.05_{(syst)} \mathrm{GeV}$$
$$m_H^{(\gamma\gamma)} = 125.11 \pm 0.21_{(stat)} \pm 0.36_{(syst)} \mathrm{GeV}$$

$$\Delta m_H = 0.23 \pm 0.42_{(stat)} \pm 0.36_{(syst)} \mathrm{GeV}$$

Combined fit:

5 independent signal strengths:
$\mu^{4\ell}, \mu^{\gamma\gamma}_{gg}, \mu^{\gamma\gamma}_{VBF}, \mu^{\gamma\gamma}_{VH}, \mu^{\gamma\gamma}_{ttH}$

Combination of $H \to 4\ell \oplus H \to \gamma\gamma$

$$m_H^{(4\ell)} = 124.88 \pm 0.37_{(stat)} \pm 0.05_{(syst)}\ \mathrm{GeV}$$
$$m_H^{(\gamma\gamma)} = 125.11 \pm 0.21_{(stat)} \pm 0.36_{(syst)}\ \mathrm{GeV}$$

$$\Delta m_H = 0.23 \pm 0.42_{(stat)} \pm 0.36_{(syst)}\ \mathrm{GeV}$$

Combined fit:

5 independent signal strengths:
$\mu^{4\ell},\ \mu^{\gamma\gamma}_{gg},\ \mu^{\gamma\gamma}_{VBF},\ \mu^{\gamma\gamma}_{VH},\ \mu^{\gamma\gamma}_{ttH}$

Main correlated systematic uncertainties:
calibration of e/γ ; pileup modelling ; luminosity

Combination of $H \to 4\ell \oplus H \to \gamma\gamma$

$$m_H^{(4\ell)} = 124.88 \pm 0.37_{(stat)} \pm 0.05_{(syst)} \text{ GeV}$$
$$m_H^{(\gamma\gamma)} = 125.11 \pm 0.21_{(stat)} \pm 0.36_{(syst)} \text{ GeV}$$

$$\Delta m_H = 0.23 \pm 0.42_{(stat)} \pm 0.36_{(syst)} \text{ GeV}$$

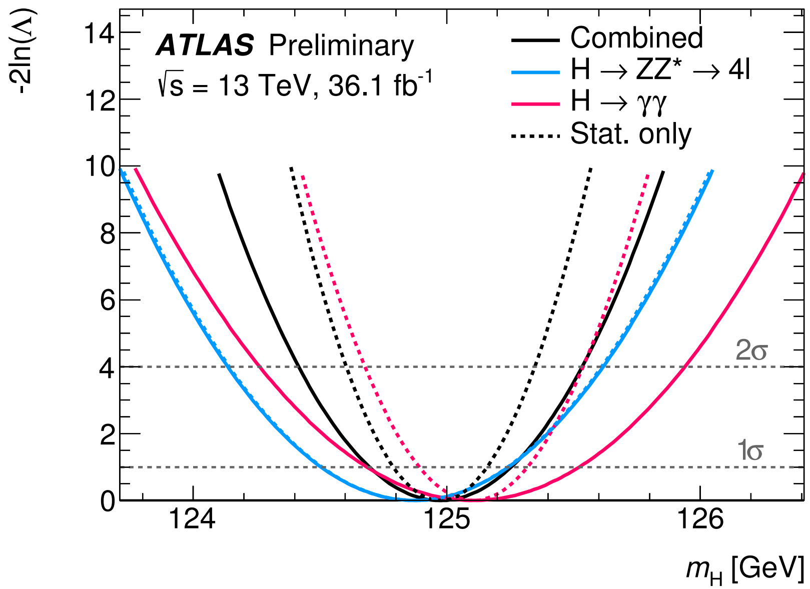

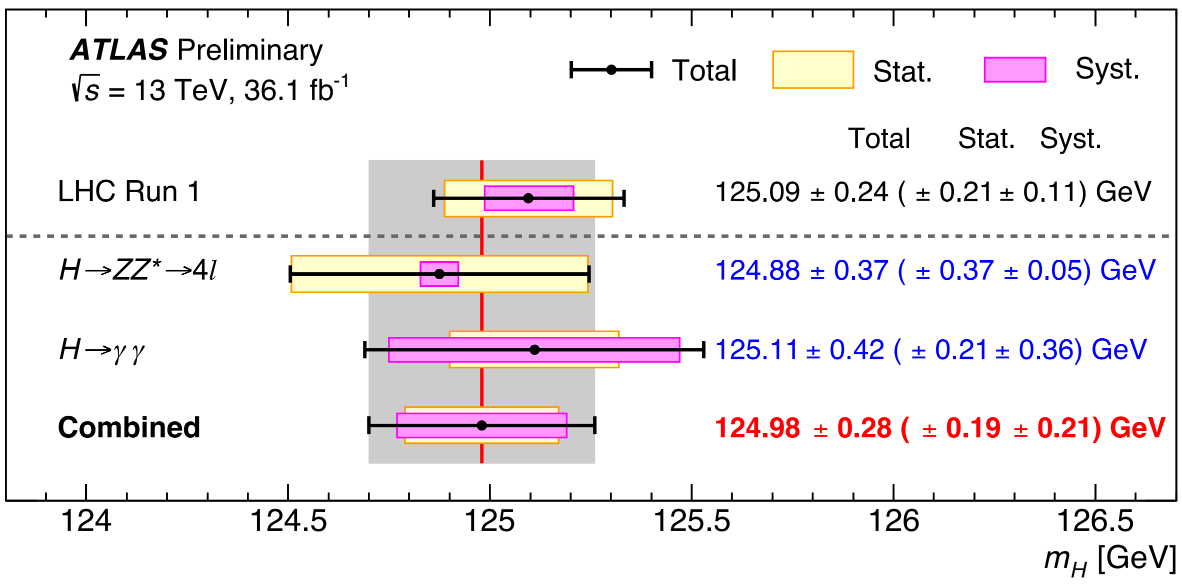

Preliminary combined Higgs mass — from ATLAS Run-II:

$$m_H = 124.98 \pm 0.19_{(stat)} \pm 0.21_{(syst)} \text{ GeV}$$

Combination of $H \to 4\ell \oplus H \to \gamma\gamma$

$$m_H^{(4\ell)} = 124.88 \pm 0.37_{(stat)} \pm 0.05_{(syst)}\ \mathrm{GeV}$$
$$m_H^{(\gamma\gamma)} = 125.11 \pm 0.21_{(stat)} \pm 0.36_{(syst)}\ \mathrm{GeV}$$

$$\Delta m_H = 0.23 \pm 0.42_{(stat)} \pm 0.36_{(syst)}\ \mathrm{GeV}$$

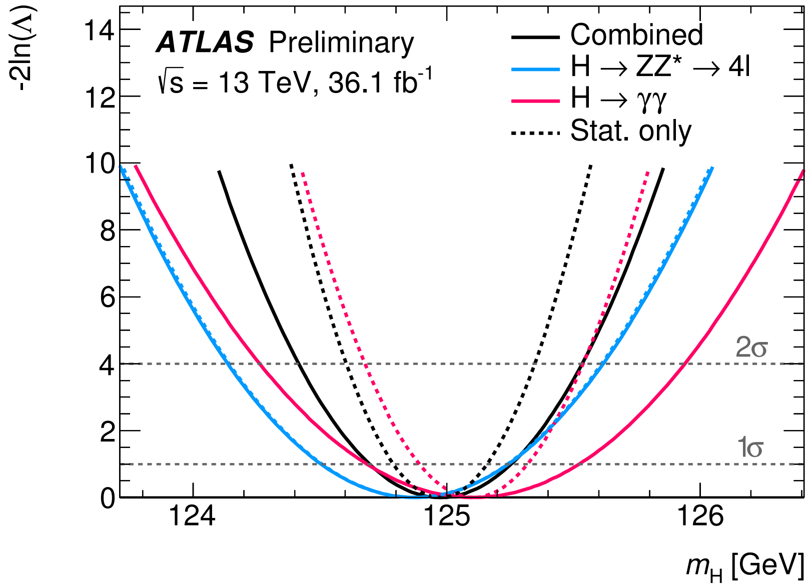

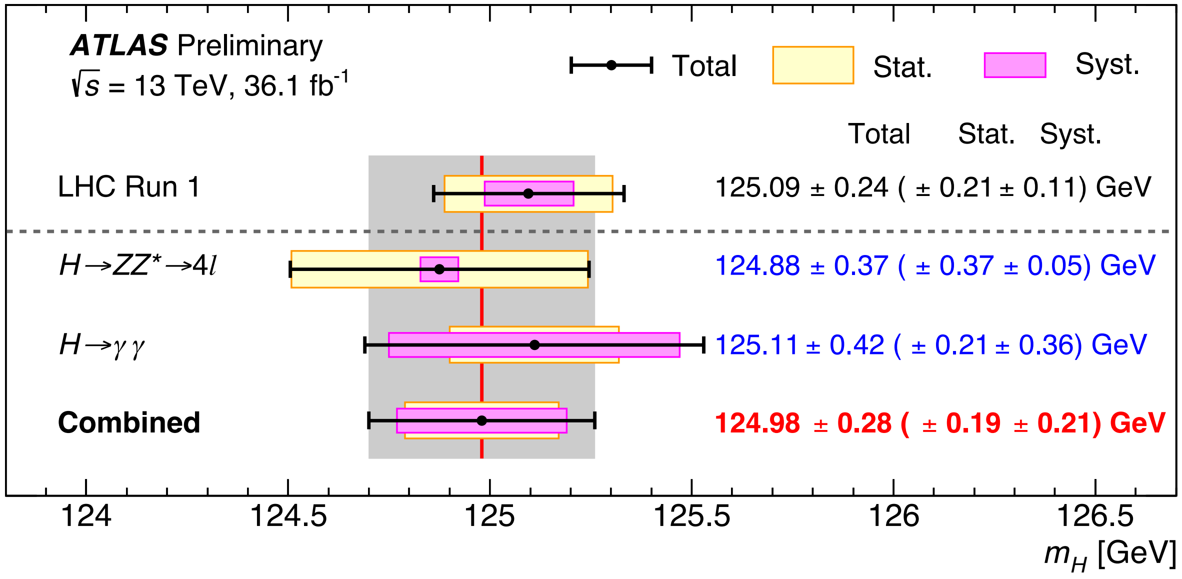

Preliminary combined Higgs mass — from ATLAS Run-II:

$$m_H = 124.98 \pm 0.19_{(stat)} \pm 0.21_{(syst)}\ \mathrm{GeV}$$

(compare with Run-1 ATLAS⊕CMS result: $m_H = 125.09 \pm 0.21_{(stat)} \pm 0.11_{(syst)}\ \mathrm{GeV}$)

BACKUP

ATLAS⊕CMS combined measurement, run-1

Using the $H \to \gamma\gamma$ and $H \to ZZ^* \to 4\ell$ decay channels
that allow a full kinematics reconstruction with good invariant mass resolution ($\mathcal{O}(1\ \mathrm{GeV})$)

(main source of systematic: energy scale)

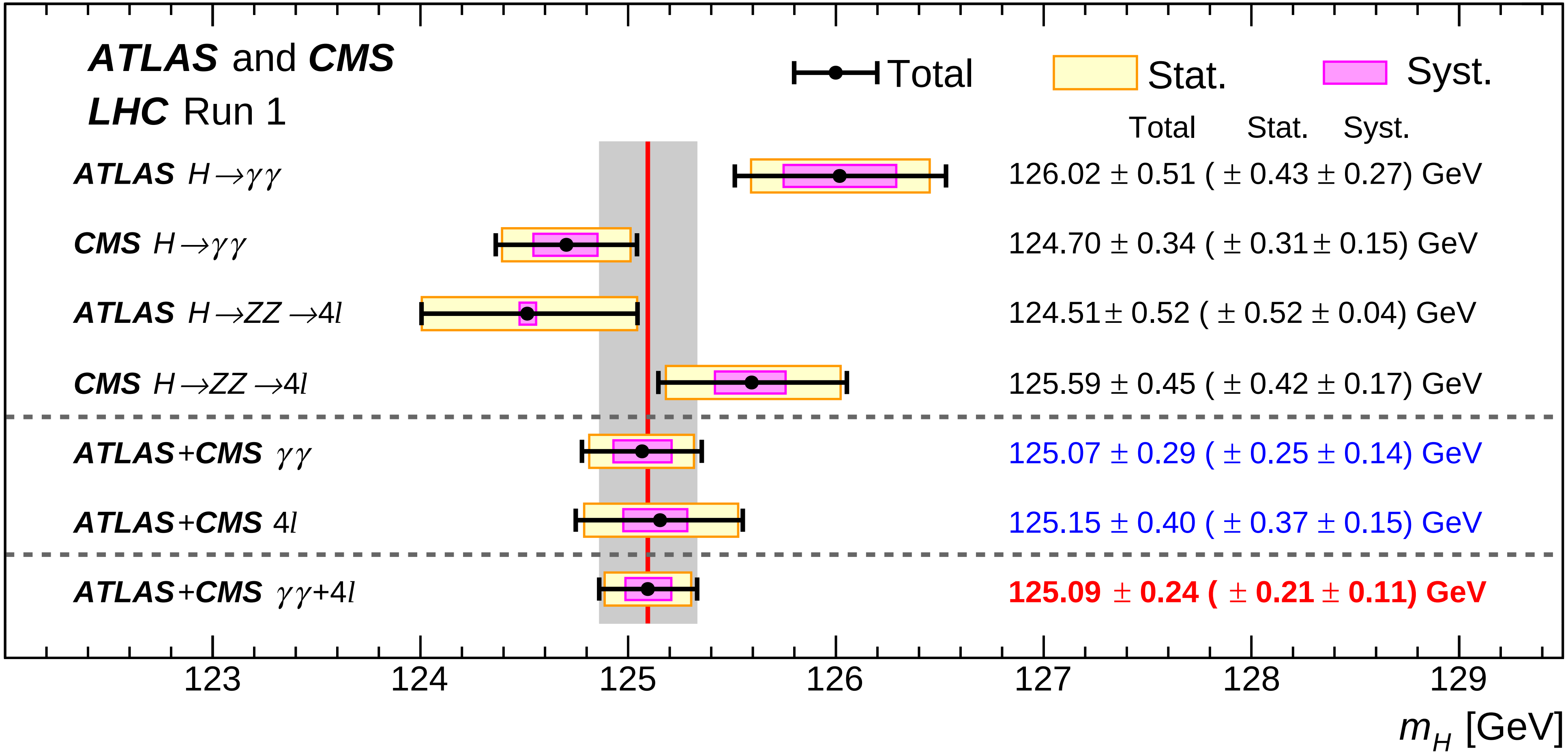

$$\hat{m}_H = 125.09 \pm 0.21(stat) \pm 0.11(syst)\ \mathrm{GeV}$$